PHYSICAL REVIEW B VOLUME 48, NUMBER 4 15 JULY 1993-II

X-ray-diffraction characterization and sound-velocity measurements of W/Ni multilayers

Eric E. Fullerton, Sudha Kumar, and M. Grimsditch
Materials Science Division, Argonne National Laboratory, Argonne, Illinois 60439

David M. Kelly and Ivan K. Schuller
Department of Physics 0319, University of California, San Diego, La Jolla, California 92093-0319
(Received 15 June 1992)

We present detailed structural characterization and shear elastic constant measurements of sputtered W/Ni multilayers. Structural refinement of the reflection x-ray-diffraction spectra was used to determine the out-of-phase lattice spacings of the constituent layers. The Ni(111) lattice spacing expands $\approx 3\%$ and the W(110) lattice spacing is constant with decreasing modulation wavelength Λ down to $\Lambda \approx 30$ Å. Transmission x-ray diffraction was used to determine the in-plane structure. The W layers undergo an anisotropic contraction in plane with the [002] directions contracting $\approx 2\%$ and the $[1\bar{1}0]$ remaining constant with decreasing Λ. The Ni $[2\bar{2}0]$ expands $\approx 1.5\%$ with decreasing Λ. The Ni layer expands both in plane and out of plane, contradicting Poisson ratio arguments relating in-plane and out-of-plane strains. Below $\Lambda = 35$ Å the multilayers undergo a structural transition in which both layers transform into a random close-packed structure. The shear velocity decreases $\approx 22\%$ with decreasing Λ down to the disorder transition and then is Λ independent. The results imply that there is a correlation between the origin of the elastic anomalies and amorphization.

I. INTRODUCTION

The elastic and structural properties of metallic multilayers have been a subject of considerable experimental[1] and theoretical[2–5] study. Much of this interest is derived from the variety of elastic anomalies observed in metallic multilayers. For instance, the measured shear moduli in Ag/Pd increases $\approx 50\%$,[6] Nb/Cu decreases $\approx 30\%$,[7] and Cu/Ni is constant[8] with decreasing modulation wavelength (Λ). Anomalies of different signs can also be present in the same system, as was demonstrated in Nb/Cu, where the biaxial modulus increases and the shear modulus decreases with decreasing Λ.[7]

In systems that show softening in the shear modulus, the softening can often be directly correlated with an expansion in the average lattice spacing $\bar{d}$.[9] It is generally accepted that the observed elastic anomalies are correlated to structural changes resulting from the interfaces. However, the nature of the structural changes and how it relates to the elastic properties is presently unresolved. A key step toward understanding the anomalous physical properties is performing a detailed structural characterization including quantitative determination of both the lattice strains and structural disorder of the constituent layers. Additional information can be obtained by studying the elastic properties of a multilayer as one of the constituent layers undergoes a structural transition.[10]

In this study we present detailed structural characterization of W/Ni multilayers by x-ray diffraction. Mo/Ni has been extensively studied[11–14] and exhibits the largest softening of the shear modulus of any system reported. This softening was directly correlated to the measured expansion of $\bar{d}$.[11] *W* was chosen to replace Mo because it is lattice matched to Mo within 0.6% but has a smaller compressibility.

X-ray diffraction in the reflection geometry is the most commonly used technique for determining the structure of multilayers.[15] Unfortunately, the information determined directly from the peak positions of the diffraction spectra are, in general, limited to averaged quantities of the constituent layers such as the modulation wavelength Λ and the average perpendicular lattice spacing $\bar{d}$. To determine the perpendicular lattice strains of the constituent layers, it is necessary to fit the diffraction spectra to model calculations. Measurements of in-plane lattice strains requires diffraction with the scattering vector in the plane of the film by transmission or grazing-incidence diffraction. In this paper, we describe both reflection and transmission x-ray diffraction of sputtered W/Ni multilayers. By combining these techniques, we obtain a complete crystallographic determination of the lattice strains as a function of Λ and show that the samples transform from a bcc/fcc multilayer into a compositionally modulated random closed-packed structure for $\Lambda < 30$ Å. These results are then correlated to elastic-constants measurements.

II. EXPERIMENTAL PROCEDURES

A series of equal-layer-thickness W/Ni multilayers (10 Å $< \Lambda < 300$ Å) and total thickness of 1 μm were prepared by magnetron sputtering onto ambient temperature sapphire and Si substrates as described earlier.[16] Sputtering rates were checked by quartz-crystal monitors before and after deposition and found to be constant within 5%. Structural studies were performed on a computer-controlled Rigaku rotating anode x-ray diffractometer using Cu Kα radiation. Shear-elastic constants were measured by Brillioun light scattering with a 5+2 tandem Fabry-Perot spectrometer.[17]

0163-1829/93/48(4)/2560(8)/$06.00

III. REFLECTION X-RAY DIFFRACTION

A. Low angle

Low-angle θ-2θ x-ray-diffraction scans were performed on the samples to characterize the chemical modulation. Shown in Fig. 1 are the low-angle diffraction spectra for the $\Lambda = 112$ and 13 Å W/Ni multilayers. Clearly resolved low-angle diffraction peaks were observed for all modulation wavelengths studied confirming the existence of a well-defined layered structure. For the $\Lambda = 112$ Å multilayer, the suppression of the even-order peaks resulting from the equal layer thickness implies a square compositional profile. Broadening of the higher-order multilayer peaks indicates some cumulative layer-thickness fluctuations. Even for the $\Lambda = 13$ Å multilayer, the third-order peak is observed, indicating that the multilayer maintains a modulated structure with chemically segregated layers. If the composition profile were sinusoidal, then only the first-order diffraction peak would be observed. The second-order diffraction peak is no longer suppressed, which most likely results from a deviation from a square compositional profile or asymmetries of the interfaces. Given that the third-order peak is observed, we estimate that the interdiffusion is limited to only the first atomic layer about the interface. A detailed analysis of the W/Ni low-angle spectra together with glancing angle x-ray-fluorescence spectra will be presented elsewhere.[18]

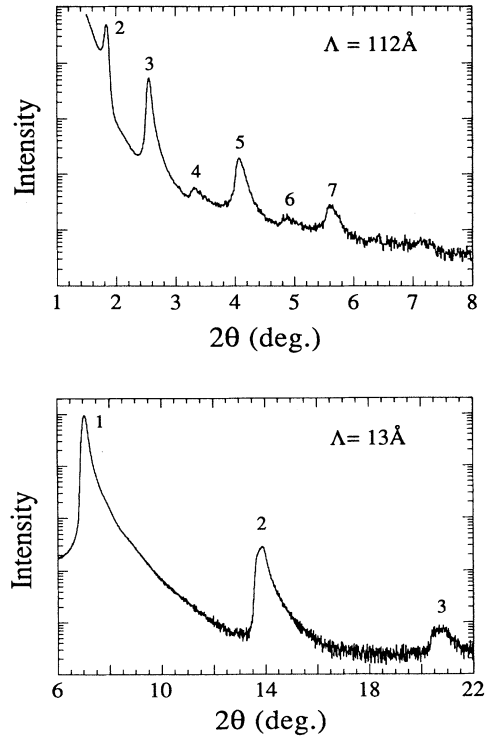

FIG. 1. Low-angle θ-2θ x-ray-diffraction spectra for $\Lambda = 112$- and 13-Å W/Ni multilayers. Numbers indicate the order of reflection.

B. High angle

Shown in Fig. 2 are the high-angle θ-2θ x-ray-diffraction spectra for a representative set of W/Ni multilayers. The multilayers are oriented bcc(110)/fcc(111) and are polycrystalline in the plane for $\Lambda > 30$ Å. Multilayer structure was observed for all the samples except the $\Lambda = 13$ Å W/Ni sample, in which only a broad peak at an intermediate position to that expected for W(110) and Ni(111) was observed. The high-angle multilayer peak positions are located about the expected Bragg positions of the constituents and are commonly indexed by the relation

$$2\frac{\sin\theta}{\lambda_x} = \frac{1}{\bar{d}} \pm \frac{n}{\Lambda} , \tag{1}$$

where λ_x is the x-ray wavelength (1.5418 Å), n is an integer that labels the order of the satellites around the main Bragg peak, and $\bar{d}$ is the average lattice spacing of the multilayer. For a general A/B multilayer, the value of $\bar{d}$ is given by

$$\bar{d} = \frac{(\bar{N}_A - 1)\bar{d}_A + (\bar{N}_B - 1)\bar{d}_B + d_{AB} + d_{BA}}{\bar{N}_A + \bar{N}_A} , \tag{2}$$

where $\bar{N}_{A(B)}$ and $\bar{d}_{A(B)}$ are the average number of atomic planes and lattice spacing, respectively, of the A (B) layer and d_{AB} and d_{BA} are the interface lattice spacings going from layer A to B and B to A, respectively.

Equation (1) implies that the only quantities that can be determined from the x-ray peak positions are $\bar{d}$ and Λ.

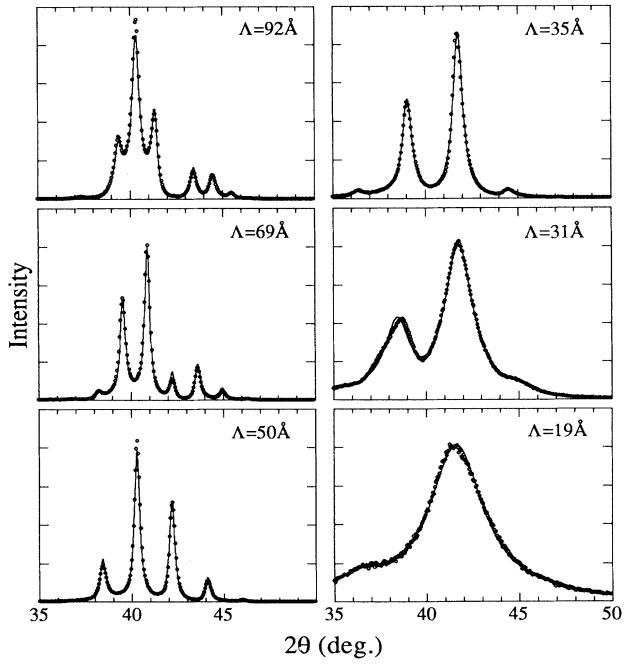

FIG. 2. High-angle θ-2θ x-ray-diffraction spectra for representative W/Ni multilayers with the scattering vector normal to the layers. The open circles are the measured points and the solid line is the result of the structural refinement procedure described in the text.

Figure 3(a) shows the measured $\bar{d}$ as a function of Λ and the expected average, calculated from the bulk lattice spacings, assuming equal layer thicknesses (dashed line). For large Λ, the measured values agree with the expected average while below $\Lambda=90$ Å there is a monotonic expansion reaching 2.1% at $\Lambda\approx 20$ Å. The estimated structural coherence length ξ determined from the measured line widths via Sherrer's equation is shown in Fig. 3(b). The coherence length of the W/Ni multilayers decreases monotonically down to the thinnest modulation with a sharp drop at $\Lambda=35$ Å. Rocking curves about the main Bragg reflections were used to determine the mosaic spread of the crystal orientations. Shown in Fig. 3(c) is the rocking-curve full width at half maximum as a function of Λ. The rocking-curve widths are relatively constant down to $\Lambda=35$ Å and then increase dramatically. For the $\Lambda=19$ and 13 Å samples, the rocking-curve widths were greater than 30 °, indicating that the films are essentially randomly oriented.

To determine the structure of the individual layers requires modeling the multilayer and comparing the calculated intensities from the modeled structure with the measured intensities. Comparing the entire experimental and calculated spectra (including relative peak intensities, line shapes, and background intensities) requires that lattice strains and structural disorder be included in the model. Fitting to the measured spectrum by iteratively adjusting the lattice and disorder parameters allows a quantitative refinement of these parameters. The details of the refinement technique, structural modeling, and discussion of the reliability of the refined parameters have been given elsewhere.[19,20]

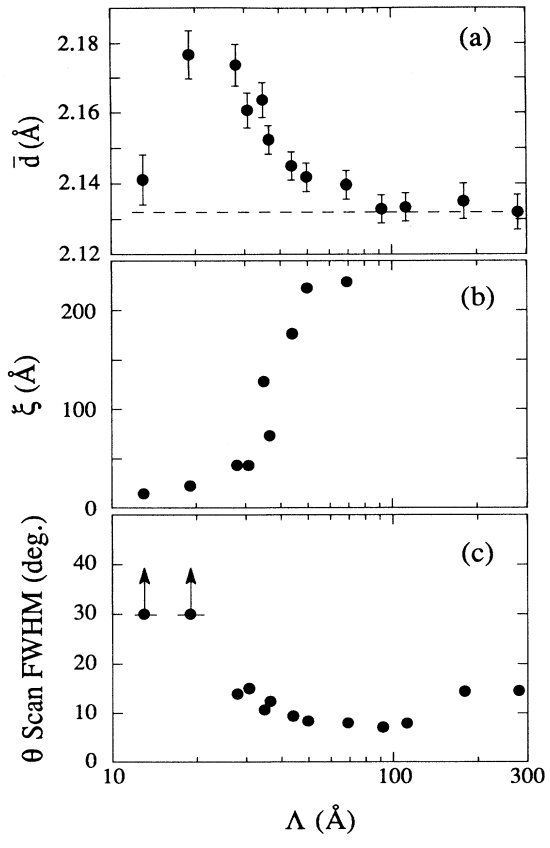

FIG. 3. Structural parameters determined from the high-angle x-ray-diffraction spectra versus Λ. (a) Perpendicular average lattice spacing $\bar{d}$. (b) Crystalline coherence length estimated from the high-angle line width. (c) Rocking-curve full width at half maximum.

The crystal-structure model from Refs. 19 and 20 was used to describe the lattice spacing within the layer. The $A(B)$ layers are modeled as having lattice spacing $d_{A(B)}$ in the center of the layer. To account for possible changes close to the interfaces the first three atomic planes at each interface were allowed to deviate from $d_{A(B)}$ by an amount $\Delta d_{A(B)}\exp(-\alpha n)$, where $n=0$, 1, and 2 for the first, second, and third atomic plane away from the interface. To allow for differences along the growth direction the values of Δd were not constrained to be the same at the top and bottom surfaces of each layer and therefore give rise to the fitting parameters Δd_1 and Δd_2 for each material. The value for α was somewhat arbitrarily kept at 0.5. Interdiffusion was modeled by setting the scattering power of the atomic planes near the interface as a weighted average of W and Ni.

The fitting parameters that can be used in our refinements are: $\bar{N}_{A(B)}$, $s_{A(B)}$, $d_{A(B)}$, $\Delta d_{A(B)1}$, $\Delta d_{A(B)2}$, c, d_{AB}, d_{BA}, as well as a constant-background parameter and another to scale the intensity. $s_{A(B)}$ are the standard deviations of the layer thickness resulting from discrete disorder for layer $A(B)$ and c is the continuous fluctuation of the interface distance as described in Ref. 19. The spectra were fitted using different subsets of parameters and starting from different initial values to avoid local minima. The three subsets of lattice constants that were fitted are (1) a uniform layer in which the strain parameters Δd_{A1}, Δd_{A2}, Δd_{B1}, and Δd_{B2}, set equal to zero, and the lattice spacing d_A and d_B, were used as fitting parameters; (2) the centers of the layers spacings were set at the large Λ values ($d_{\mathrm{W}}=2.238$ Å and $d_{\mathrm{Ni}}=2.035$ Å) and the strain parameters were fitted; and (3) all the lattice spacings were allowed to vary. The interface spacings d_{AB} and d_{AB} were not used as a fitting parameters but were set at the average value of the nearest A and B atomic spacings. For $\Lambda=19$ Å and samples with $\Lambda>70$ Å, only model (1) was used.

The solid lines in Fig. 2 are the calculated spectra using the parameters of the refinement procedure. There is excellent agreement in peak position, relative peak intensity, and line shape for all the samples. The discrete roughness of the layers was in general small (≈ 1–2 Å) for the smaller modulations ($\Lambda<70$ Å) and increased for larger Λ. The continuous roughness per interface, c, was almost modulation independent down to $\Lambda\approx 35$ Å with a value of $c\approx 0.25$ Å, indicating that the disorder per interface does not significantly change. For $\Lambda<35$ Å there is a sharp increase in c to 0.45 Å, indicating an increased crystalline disorder present at the interface. This type of "disorder transition" (a sudden reduction in the structural coherence and increase in continuous disorder) has been observed in other lattice-mismatched multilayers but usually occurs at somewhat smaller modulations ($\Lambda\approx 20$ Å). An interdiffusion of $\sim 30\%$ in the first

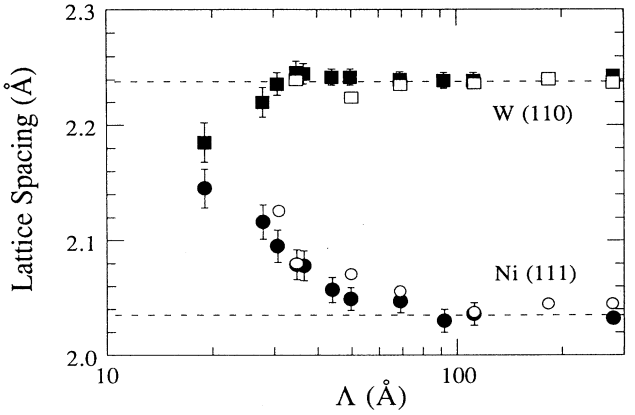

FIG. 4. Average W(110) lattice spacing (squares) and Ni(111) lattice spacing (circles) determined by x-ray refinement (solid symbols) and transmission x-ray diffraction (open circles).

monolayer at each interface gave the best fits.

The perpendicular W and Ni lattice spacings (solid symbols) obtained from fitting the x-ray spectra are shown in Fig. 4. The average lattice spacing $\bar{d}$ [calculated from Eq. (2)] is consistent with that obtained directly from the central peak position in the spectra in Fig. 2. The results show that most of the expansion is in the Ni layers; this is consistent with previous work on Nb/Cu and Mo/Ni multilayers,[1] where it was also found that the fcc material changes most drastically. Only at the smallest Λ's (<30 Å) is there a small change in the bcc lattice constant, a contraction of W in this case.

The fact that the Ni and not the W layers expand is clearly established from the refinement results. The distribution of the expansion within the Ni layer is a more subtle question. Some insight into the origin of the lattice expansion can be found by examining the refined values of the strain parameters. Because of some interdependency between the fitting parameters d_A, Δd_{A1}, and Δd_{A2}, for a given layer, the uncertainty of these values tends to be larger than the uncertainty in $\bar{d}_A$. When model (2) or (3) was used, the value of Δd_{Ni1} was consistently found to be expanded with an average value of $\Delta d_{\mathrm{Ni1}}=0.13\pm0.05$ Å for the 28 Å $<\Lambda<$ 70 Å samples. The uncertainties represent the standard deviations of the lattice strain parameters for the different samples and for different fitting parameters. For comparison, the other strain parameters were determined to be much smaller: $\Delta d_{\mathrm{W1}}=0.01\pm0.05$ Å, $\Delta d_{\mathrm{W2}}=0.03\pm0.05$ Å, and $\Delta d_{\mathrm{Ni2}}=0.04\pm0.05$ Å. The results imply that much of the expansion results from the growth of Ni on W and that the interfaces are not symmetric.

IV. TRANSMISSION X-RAY DIFFRACTION

To study the in-plane structure of the multilayer, W/Ni samples were removed from the substrate and supported on kapton sheets. X-ray-diffraction scans were performed in a transmission geometry with χ, the angle that the scattering vector subtends with the film normal, set to 90 °, 70.5 °, 54.7 °, and 45 °. The in-plane $\chi=90$ ° scans for some selected W/Ni multilayers are shown in Fig. 5. Because W and Ni have different crystal symmetries and are not lattice matched, the transmission diffraction peaks are characteristic of the individual constituent layers. The diffraction peaks were fitted to modified Lorentzian line shapes to determine the peak positions. The expected peaks corresponding to directions perpendicular to the W(110) and Ni(111) growth directions are observed and their expected positions are labeled by dashed lines. The measured in-plane lattice spacings for the principal W directions ([$1\bar{1}0$)] and [002]) are shown in Fig. 6(a). The W[$1\bar{1}0$] spacing is constant at the bulk value to within 0.2% down to $\Lambda=30$ Å. The W[002] spacing, on the other hand, contracts monotonically as Λ is reduced and reaches a -2.2% strain in the $\Lambda=28$ Å sample. Because of the polycrystalline nature of the samples it is not possible to directly measure the angle between the [$1\bar{1}0$] and [002] directions. If, however, they were not orthogonal the ($1\bar{1}2$) and the ($\bar{1}12$) in-plane spacings would be inequivalent and a doublet should be observed in the spectra. The absence of a doublet, or indeed of any additional broadening of the [$1\bar{1}2$] peak relative to the [$1\bar{1}0$] and [002] peaks, allows us to conclude that the [$1\bar{1}0$] and [002] directions remain essentially orthogonal. The measured [$1\bar{1}2$] strain agrees with that calculated from the [$1\bar{1}0$] and [002] strains assuming they are orthogonal. Because the W[$1\bar{1}2$] and Ni[$2\bar{2}0$] spacings differ by only 3.7%, their reflections almost overlap and, since the W scattering power is much higher than that of Ni, the Ni[$2\bar{2}0$] peak is difficult to resolve at small Λ. The Ni[$2\bar{2}0$] spacings were therefore determined by fitting the W[$1\bar{1}2$] and Ni[$2\bar{2}0$] peaks to a superposition of two lines. The results of the fitting are given in Fig. 6(a) (open circles) and show that the in-plane

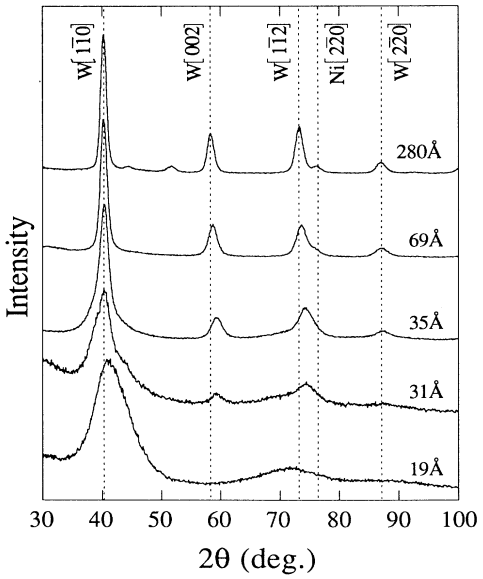

FIG. 5. Transmission ($\chi=90$ °) θ-2θ x-ray-diffraction spectra for selected W/Ni multilayers. Dashed lines indicate expected position of Bragg reflections perpendicular to the W(110) and Ni(111) directions.

Ni spacing expands with decreasing Λ to $\approx 1.5\%$ for the $\Lambda = 35$ Å sample.

The anisotropic strain of the W layer is not surprising, given the different in-plane symmetries of W and Ni. The expected in-plane orientation is Nishiyama-Wasserman[21] with the W[001]-Ni[$1\bar{1}0$] and the W[$1\bar{1}0$]-Ni[$11\bar{2}$] directions aligned. The spacing mismatches along these directions are 26% and 3%, respectively. The large difference in lattice mismatch most likely gives rise to the anisotropic strain. Similar anisotropic strains have been observed in the Nb layer of Nb/Cu multilayers[22] and the Mo layer in Mo/Ni multilayers.[14]

Shown in Fig. 6(b) are the results for the W[112] and [200] spacings and the Ni [200] and [$1\bar{1}1$] spacings, which were measured at $\chi = 54.7°$, 45°, 54.7°, and 70.5°, respectively. For these scans, the coherence length is limited to the layer thickness so for small Λ, the peaks are very broad and the positions are difficult to determine with high accuracy. The W[200] spacings are nearly Λ independent down to $\Lambda = 35$ Å, contracting only 0.3%, whereas the W[112] contracts $\approx 1.0\%$. The Ni layer expands along both the [$1\bar{1}1$] and [200] directions.

The results of the transmission scans can be used to calculate the out-of-plane spacings.[22] The same arguments as were made for the in-plane results allow us to ascertain that the W[110], [$1\bar{1}0$], and [002] directions remain orthogonal. Under these conditions the following relations between the W lattice spacings can be written:

$$\frac{1}{d^2_{110}} = \frac{1}{d^2_{112}} - \frac{1}{d^2_{002}} , \tag{3}$$

$$\frac{1}{d^2_{110}} = \frac{1}{d^2_{200}} - \frac{1}{d^2_{1\bar{1}0}} . \tag{4}$$

These equations allow for two independent estimates of the out-of-plane W(110) spacing. For $\Lambda > 30$ Å, the results of Eqs. (3) and (4) agree within 0.3% and are given by the open squares in Fig. 4. These results are in excellent quantitative agreement with the refinement results showing a Λ-independent W(110) lattice spacing.

In the analysis of the Ni in-plane [$2\bar{2}0$] peak, which is close to an intense W peak, our results are not accurate enough to enable a reliable determination if the {$2\bar{2}0$} directions are equivalent. However, the absence of doublets in the out-of-plane [200] and [$1\bar{1}0$] peaks again provides evidence that the in-plane [$2\bar{2}0$] directions are equivalent and orthogonal to the [111] growth direction. Under these conditions the following relations between lattice spacings hold:

$$\frac{1}{d^2_{111}} = 3\left[\frac{1}{d^2_{002}} - \frac{1}{d^2_{1\bar{1}1}}\right] , \tag{5}$$

$$\frac{1}{d^2_{2\bar{2}0}} = \frac{4}{d^2_{1\bar{1}1}} - \frac{1}{d^2_{002}} . \tag{6}$$

The results from Eq. (6) for the Ni[$2\bar{2}0$] spacings are shown as the open squares in Fig. 6(a). The calculated Ni[$2\bar{2}0$] strains are in reasonable agreement with the measured values, showing the same in-plane expansion with decreasing Λ. The results of Eq. (5) for the Ni(111) spacings are given by the open circles in Fig. 4. As was found for the W layer, there is excellent agreement between the refined and calculated values, showing an expansion in the Ni layer.

For modulation wavelengths larger than 35 Å, the structural characterization of our W/Ni multilayers indicates that each material is close to its bulk structure and textured growth direction, but that each material is strained anisotropically so that the symmetry of each constituent is no longer cubic. W is strained anisotropically in the plane with the [$1\bar{1}0$] direction, retaining its bulk value and the [002] axis contracting by $\approx 2\%$; perpendicular to the layers the W[110] spacing shows only a marginal contraction at the smallest Λ. The Ni layers are strained isotropically in plane and expand by $\approx 1.5\%$; they also expand by $\approx 3\%$ perpendicular to the layers. This volume expansion of Ni contradicts simple models that assume that the driving forces for the lattice strains are in-plane "coherency type" which, through Poisson's ratio, require the in- and out-of-plane strains to have opposite sign.[22]

Below $\Lambda = 35$ Å significant structural changes occur that cannot simply be described by strains. From the refinement results of the $\chi = 0$ spectra, there is a large increase in the continuous roughness and a considerable shift in the peak identified as W[110]. Additionally, the rocking curves show that the samples lose their preferred

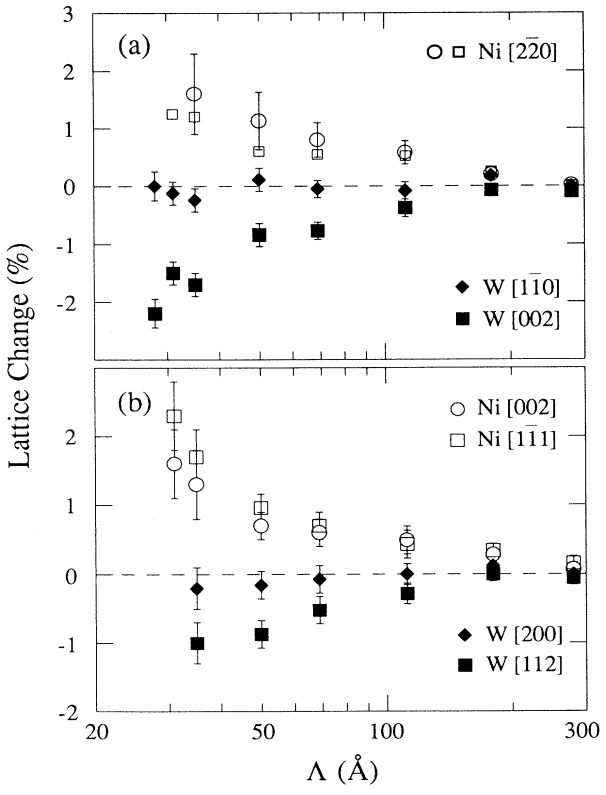

FIG. 6. Transmission x-ray-diffraction results for different crystallographic orientations. (a) In-plane $\chi = 90°$ results. The open squares are calculated from the results in (b). (b) $\chi = 70.5°$, 54.7°, and 45° results.

crystal orientation. The in-plane ($\chi=90$ °) scans similarly show an abrupt change below $\Lambda=35$ Å. The $\Lambda=31$ Å sample shows an asymmetry towards higher angles of the $W[1\bar{1}0]$ peak and a decrease of the W[002] and W[$1\bar{1}2$] intensities; furthermore, an additional broad peak at $2\theta\approx71$ ° begins appearing. For the $\Lambda=19$ Å sample, the W[002] and [$1\bar{1}2$] are no longer observed. There is only a broad, slightly asymmetric peak at $\Lambda\approx41$ ° and a broad peak at $2\theta\approx71$ °. The increasing intensity at lower angles results from the kapton sheet supporting the film. From the $\chi=70.5$ °, 54.7 °, and 45 ° scans on this sample, peaks are also observed at $2\theta\approx42$ ° and 71°. The low-angle spectra, however, show that even at $\Lambda=13$ Å the samples retain a chemical modulation.

The x-ray spectra from multilayers with $\Lambda<20$ Å that show the broad peaks at 42 ° and 71 ° are consistent with the [111] and [220] spacings of an fcc lattice in which the grain size is 10–25 Å. This identification, however, is inconsistent with the absence of a peak corresponding to the [200] direction. In Fig. 7 we compare the $\chi=90$ ° spectrum from our $\Lambda=19$ Å sample with that from amorphous $Fe_{80}P_{13}C_7$, which is believed to have a random close-packed structure (rcp).[23] (The $Fe_{80}P_{13}C_7$ spectrum has been normalized along the 2θ axis to account for the difference in atomic size as well as the x-ray wavelength used in the experiments). The similarity between the spectra is almost perfect, even reproducing the weak shoulder at ~90 °. The identification of the structure as rcp also explains why spectra recorded at different values of χ are essentially identical.

The slight change in the first rcp peak positions for different values of χ results from the difference in the atomic distances in the W and Ni layers. The $\chi=90$ ° scan records each layer independently, so the spectrum should be dominated by the W layer, which is a stronger scatterer. Therefore, the peak position at $2\theta\approx41$ ° should correspond to the W spacings (≈2.2 Å), which agree with refined value in Fig. 4. The $\chi=0$ ° scan averages over both layers so the peak position should be an average of the W and Ni spacings (2.175 Å). This allows for an estimate of the Ni spacing of ≈2.15 Å which is also in agreement with the refinement results.

The above identification of the rcp structure of small modulation wavelength W/Ni multilayers is consistent with previous reports of disordered[11] and amorphous[24–26] structures below a critical Λ. We would like to stress that this amorphous phase is not present at the interface of the $\Lambda>35$ Å samples. It is well known that multilayers with amorphous interfaces (e.g., Ti/Ni) results in the crystal-coherence length being limited to the individual layer thicknesses and in the loss of high-angle multilayer peaks.[12,15,26]

V. ELASTIC PROPERTIES

Shown in Fig. 8 is the measured velocity of the surface acoustic phonon versus Λ for the W/Ni multilayers. The phonon velocity is related to the shear modulus C_{44} by the relation

$$v=\beta\sqrt{C_{44}/\rho} \tag{7}$$

where ρ is the average density of the multilayer and β ($\approx0.8-1.0$) is a constant which depends weakly on C_{11}, C_{33}, and C_{13}. (All C_{ij} are in the coordinate system of the multilayer and not in that of the constituents).[27]

The measured velocity can be directly compared to velocities calculated using continuum elasticity theory. The elastic constants of the multilayer entering the calculation are determined from bulk W and Ni values given in the literature. In order to allow comparison with any future elastic measurements on this system, we list in Table I the in-plane-averaged elastic constants of W, Ni, and W/Ni. Since W is, fortuitously, elastically isotropic, the Reuss (R) and Voigt (V) averages are identical. The elastic constants of the multilayer were calculated from the expressions in Ref. 27. The Rayleigh wave velocities calculated from these constants are $v^V=2.53$ and $v^R=2.38$ km/sec; they are shown by the arrows in Fig. 8. At large Λ, the measured velocities agree with the calculated values. As Λ decreases, the phonon velocity decreases to $\Lambda\approx35$ Å, below which the velocity is nearly Λ independent. The total decrease in the velocity is ~22%.

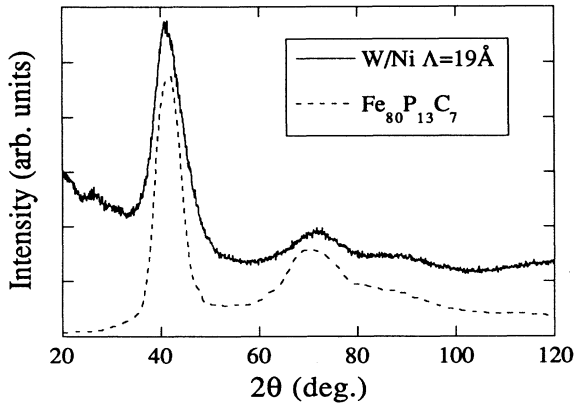

FIG. 7. $\chi=90$ ° scan of $\Lambda=19$ Å multilayer compared to the x-ray scan of a $Fe_{80}P_{13}C_7$ sample with random closed-pack structure.

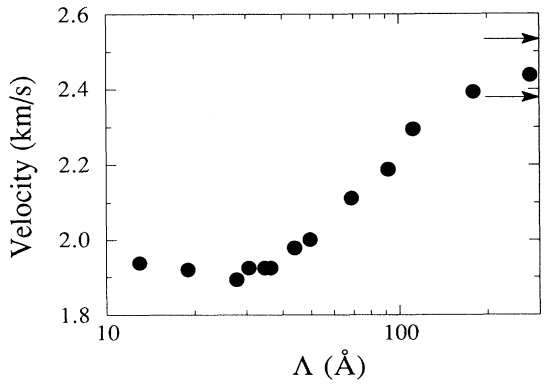

FIG. 8. Surface acoustic-phonon velocity vs Λ. Arrows indicate calculated velocities for Voigt (upper) and Reuss (lower) averages.

TABLE I. Elastic constants (GPa) of (110) textured W, (111) textured Ni, and W/Ni multilayers. *V* and *R* indicate the Voigt and Reuss averages (in W they are identical).

Elastic constant	W	Ni^V	Ni^R	W/Ni^V	W/Ni^R
$C_{11}=C_{22}$	517	322	305	414	405
C_{12}	203	128	145	160	168
C_{33}	517	347	347	415	415
$C_{13}=C_{23}$	203	103	103	143	143
$C_{44}=C_{55}$	157	72	59	99	86
C_{66}	157	97	80	127	119

VI. DISCUSSION

Even with the complete structural characterization of the multilayer given above, it is still not possible to uniquely correlate the structural and elastic anomalies in this system. There are, in general, two likely origins for the anomalous properties of the shear modulus: (i) decreased bonding of the atomic layers with increased lattice expansion, and (ii) stacking faults at an incoherent interface facilitating a shear displacement. Most theoretical studies of elastic anomalies have concentrated on the former, where the models differ in the origin of the lattice expansions. Structural models have attributed the lattice changes to stresses present at the interfaces resulting from coherency strains[3] or surface tensions.[5] A recently proposed electron-transfer model has also predicted lattice expansions.[4]

The identification of the transformation to an rcp structure for thin layers gives some insight into the origin of the softening in the shear modulus. Extensive work has been done on the effects of ion irradiation on the shear modulus of different materials.[28–30] A particularly relevant example is ion-beam damage in Zr_3Al.[30] As the ion fluence increases, disorder induced in the Zr_3Al gives rise to a net atomic-volume expansion and a commensurate decrease in the shear modulus. At a critical dose, the material undergoes a crystalline-amorphous transition where the shear modulus increases slightly and becomes independent of further irradiation. This is in qualitative agreement with what is observed in the W/Ni system as Λ is decreased. There is a volume expansion of the Ni layer (of $\approx 6\%$ compared to 3% for Zr_3Al), a large decrease in the shear-wave velocity (22% compared to 32% for Zr_3Al), and a transition to an amorphous phase that has a constant shear-wave velocity. This may imply that the origin of the softening is the same and that the large lattice mismatch at each interface introduces atomic disorder into the structure. As Λ is decreased, the defect concentration increases until the system undergoes a crystalline-to-amorphous transition. This transition is signaled by the large increase in the continuous disorder below $\Lambda = 35$ Å. This interpretation is in agreement with recent discussion of defect-induced amorphization by Fecht,[34] in which he proposes that an isentropic condition limits the stability of a crystal as a function of defect concentration. At low temperatures, above a critical defect concentration, it is expected that the crystal will undergo a crystalline-to-amorphous transition.

There has been an extensive series of theoretical modelings of lattice-mismatched multilayers using molecular dynamics by Wolf and co-workers.[2,31–33] These models have attempted to explain the effects of atomic-level disorder at the interface on the structural and elastic properties of multilayers. These results are calculated for fcc/fcc multilayers, where disorder is introduced by rotating the interfaces to form grain boundaries and/or having lattice mismatch between layers. Direct quantitative comparisons with the W/Ni results are not possible, since the calculations are not for bcc/fcc systems. However, qualitative comparisons are possible. The model calculations are generally separated into coherent and incoherent interfaces. A coherent interface requires a one-to-one correspondence of atoms across the interface. The incoherent interface results in local rearrangement of the atoms in plane, but on average, the atomic spacing remains close to the bulk values. Clearly, for $\Lambda \geq 35$ Å, where the in-plane lattice spacings differ by less than 2% from the bulk values, which is much smaller than the lattice mismatch, the incoherent case appears valid. The results of the modeling indicate that both the interface disorder and lattice expansion contribute to the elastic anomalies.

The model calculations find that for an incoherent interface, the increased structural disorder near the interface results in a volume expansion of the constituent materials proportional to the amount of interface disorder. Because of the incoherency of the interface, the in-plane lattice spacings are close to bulk values with most of the expansion in the direction normal to the film and concentrated near the interface. This result is in qualitative agreement with what is observed in the Ni layer, which appears to expand off the W layer. Although it not possible to make quantitative comparisons, the molecular-dynamics calculations appear to be in qualitative agreement with the W/Ni elastic and structural properties.

ACKNOWLEDGMENTS

This work was supported by the U. S. Department of energy under Contract No. W-31-109-ENG-38 (ANL) and DE-FG03-87ER-45332 (UCSD) and by the Office of Naval Research under Contract No. N00014-91J-1177 (UCSD).

[1]For a recent review, see I. K. Schuller, A. Fartash, E. E. Fullerton, and M. Grimsditch, in *Thin Films: Stresses and Mechanical Properties III*, edited by W. D. Nix, J. C. Brauman, E. Arzt, and L. Ben Freund, MRS Symposia Proceedings No. 239 (Materials Research Society, Pittsburgh, 1992), p. 499; I. K. Schuller, A. Fartash, and M. Grimsditch, MRS Bulletin **XV** (10), 33 (1990); R. G Brandt, Mater. Sci. Eng. B **6**, 95 (1990).

[2]D. Wolf and J. F. Lutsko, Phys. Rev. Lett. **60**, 1170 (1988).

[3]A. F. Jankowski, J. Mater. Sci. Eng. B **6**, 191 (1991).

[4]M. L. Huberman and M. Grimsditch, Phys. Rev. Lett. **62**, 1403 (1989).
[5]F. H. Streitz, K. Sieradzki, and R. C. Cammarata, Phys. Rev. B **41**, 12 285 (1990).
[6]J. Dutcher, S. Lee, J. Kim, G. I. Stegeman, and C. M. Falco, Phys. Rev. Lett. **65**, 1231 (1990).
[7]A. Fartash, E. E. Fullerton, I. K. Schuller, S. Bobbin, R. C. Cammarata, and M. Grimsditch, Phys. Rev. B **44**, 13 760 (1991).
[8]J. Mattson, R. Bhadra, J. B. Ketterson, M. B. Brodsky, and M. Grimsditch, J. Appl. Phys. **67**, 2873 (1990).
[9]I. K. Schuller and M. Grimsditch, J. Vac. Sci. Technol. B **4**, 1444 (1986).
[10]Eric E. Fullerton, Ivan K. Schuller, F. T. Parker, K. Svinarich, G. Eesley, R. Bhadra, and M. Grimsditch, J. Appl. Phys. **73**, 7370 (1993).
[11]M. R. Khan, C. S. L. Chun, G. P. Flecher, M. Grimsditch, A. Kueny, C. M. Falco, and I. K. Schuller, Phys. Rev. B **27**, 7186 (1983).
[12]B. M. Clemens and G. L. Eesley, Phys. Rev. Lett. **61**, 2356 (1988).
[13]J. L. Makous and S. M. Hues, Phys. Rev. B **44**, 10 848 (1991).
[14]J. A. Bain, L. J. Chyung, S. Brennan, and B. M. Clemens, Phys. Rev. B **44**, 1184 (1991).
[15]D. B. McWhan, in *Physics, Fabrication and Applications of Multilayered Structures,* edited by P. Dhez and C. Weisbuch (Plenum, New York, 1988) p. 67.
[16]For an early description, see I. K. Schuller, Phys. Rev. Lett. **44**, 1597 (1980).
[17]J. R. Sandercock, in *Light Scattering in Solids III,* Topics in Applied Physics Vol. 51, edited by M. Cardona and G. Güntherodt (Springer, New York, 1982).
[18]K. Huang, P. A. Montano, M. Grimsditch, E. E. Fullerton, J. M. Bai, D. Kelly, and I. K. Schuller (unpublished).
[19]E. E. Fullerton, I. K. Schuller, H. Vanderstraeten, and Y. Bruynseraede, Phys. Rev. B **45**, 9292 (1992).
[20]I. K. Schuller, E. E. Fullerton, H. Vanderstraeten, and Y. Bruynseraede, in *Structure/Property Relationsips for Metal/Metal Interfaces,* edited by A. D. Romig, D. E. Fowler, and P. D. Bristowe, MRS Symposia Proceedings No. 229 (Materials Research Society, Pittsburgh, 1991), p. 41.
[21]L. A. Bruce and H. Jaeger, Philos. Mag. A **38**, 223 (1978).
[22]A. Fartash, M. Grimsditch, E. E. Fullerton, I. K. Schuller, Phys. Rev. B **47**, 12 813.
[23]Y. Waseda and T. Masumoto, Z. PHys. B **22**, 121 (1975).
[24]B. M. Clemens, Phys. Rev. B **33**, 7615 (1986).
[25]W. J. Meng, G. L. Eesley, and K. A. Svinarich, Phys. Rev. B **42**, 4881 (1990).
[26]B. M. Clemens and R. Sinclair, MRS Bulletin **15**(2), 19 (1990) and references therein.
[27]M. Grimsditch, Phys. Rev. B **31**, 6818 (1985).
[28]P. R. Okamoto, L. E. Rehn, J. Pearson, R. Bhadra, and M. Grimsditch, J. Less-Common Met. **140**, 231 (1988).
[29]S. Koike, P. R. Okamoto, L. E. Rehn, R. Bhadra, M. Grimsditch, and M. Meshi, in *Beam-Solid Interactions: Physical Phenomena,* edited by J. A. Knapp, P. Brgesen, and A. Raymond, MRS Symposia Proceedings No. 157 (Materials Research Society, Pittsburgh, 1990), p. 777.
[30]L. E. Rehn, P. R. Okamoto, J. Pearson, R. Bhadra, and M. Grimsditch, Phys. Rev. Lett. **59**, 2987 (1987).
[31]J. A. Jaszczak and D. Wolf, J. Mater. Res. **6**, 1207 (1991).
[32]J. A. Jaszczak, S. R. Phillpot, and D. Wolf, J. Appl. Phys. **68**, 4573 (1990).
[33]D. Wolf, Mater. Sci. Eng. A **126**, 1 (1990).
[34]H. J. Fecht, Nature **356**, 133 (1992).